Neuron, Vol. 43, 729–743, September 2, 2004, Copyright ©2004 by Cell Press

Neuronal Synchrony Mediated by Astrocytic Glutamate through Activation of Extrasynaptic NMDA Receptors

Tommaso Fellin,[1,3] Olivier Pascual,[2,3] Sara Gobbo,[1] Tullio Pozzan,[1] Philip G. Haydon,[2] and Giorgio Carmignoto[1,*]
[1]Istituto CNR di Neuroscienze and
Dipartimento di Scienze Biomediche Sperimentali
Università di Padova
viale G. Colombo 3
35121 Padova
Italy
[2]Department of Neuroscience
University of Pennsylvania
School of Medicine
215 Stemmler Hall
3610 Hamilton Walk
Philadelphia, Pennsylvania 19104

Summary

Fast excitatory neurotransmission is mediated by activation of synaptic ionotropic glutamate receptors. In hippocampal slices, we report that stimulation of Schaffer collaterals evokes in CA1 neurons delayed inward currents with slow kinetics, in addition to fast excitatory postsynaptic currents. Similar slow events also occur spontaneously, can still be observed when neuronal activity and synaptic glutamate release are blocked, and are found to be mediated by glutamate released from astrocytes acting preferentially on extrasynaptic NMDA receptors. The slow currents can be triggered by stimuli that evoke Ca^{2+} oscillations in astrocytes, including photolysis of caged Ca^{2+} in single astrocytes. As revealed by paired recording and Ca^{2+} imaging, a striking feature of this NMDA receptor response is that it occurs synchronously in multiple CA1 neurons. Our results reveal a distinct mechanism for neuronal excitation and synchrony and highlight a functional link between astrocytic glutamate and extrasynaptic NMDA receptors.

Introduction

The N-methyl-D-aspartate receptors (NMDARs) (Dingledine et al., 1999) play key roles in physiopathological phenomena, such as synaptic transmission, long-term potentiation (LTP) (Bliss and Collingridge, 1993), activity-dependent refinement of synaptic connections (Bourne and Nicoll, 1993; Constantine-Paton et al., 1990), excitotoxic neuronal damage (Choi and Rothman, 1990), and epilepsy (Dingledine et al., 1990). NMDARs are heteromeric complexes assembled from NR1 and different NR2 subunits that confer to the NMDAR distinct pharmacological and kinetic properties (Dingledine et al., 1999). Depending on the subunit composition, the subcellular distribution of the NMDAR is substantially different; after the peak of synaptogenesis, the NR1/NR2A complex, characterized by rapid offset kinetics, dominates at the synapse, while the NR1/NR2B complex, characterized by slow kinetics, is mainly in extrasynaptic membrane (Rumbaugh and Vicini, 1999; Stocca and Vicini, 1998; Tovar and Westbrook, 1999). The activation of extrasynaptic NMDARs by glutamate escaping from the synaptic cleft during episodes of high synaptic activity (Conti and Weinberg, 1999; Kullmann, 1999) suggests the hypothesis that they have a distinct role (Hardingham et al., 2002; Scimemi et al., 2004; Tovar and Westbrook, 2002).

Extrasynaptic NMDARs might also represent preferential targets of glutamate released from a nonsynaptic source, such as astrocytes. These glial cells release glutamate through a Ca^{2+}-dependent mechanism (Araque et al., 2000; Bezzi et al., 1998; Parpura et al., 1994; Pasti et al., 1997, 2001), thus establishing active, reciprocal interactions with neurons (Carmignoto, 2000; Haydon, 2001). In the hippocampus, astrocytic glutamate modulates inhibitory transmission (Kang et al., 1998; Liu et al., 2004) and increases the frequency of spontaneous α-amino-3-hydroxy-5-methyl-4-isoxazolepropionic acid receptor (AMPAR)-mediated events in pyramidal neurons (Fiacco and McCarthy, 2004), probably through activation of presynaptic metabotropic glutamate receptors (mGluRs). While these studies demonstrate the influence of glutamate released from glial cells on specific events in neuronal transmission, the general role of this process as a widespread phenomenon in the brain remains to be discovered.

Here we show that activation of $[Ca^{2+}]_i$ elevations in astrocytes by various stimuli elicits in CA1 pyramidal neurons repetitive, NMDAR-mediated responses mainly due to the NR1/NR2B complex. A striking feature of this response is that it occurs with a high degree of synchrony in multiple neurons.

Results

Schaffer Collateral Stimulation Evokes Slow Inward Currents Mediated by NMDA Receptors

Intense stimulation of neuronal afferents is commonly used to study LTP, a long-lasting increase in the response of the postsynaptic neuron that is believed to represent learning and memory processes at the cellular level (Bliss and Collingridge, 1993). In hippocampal slices, in 6 of 22 CA1 pyramidal neurons tested, high-frequency stimulation of Schaffer collaterals (SCs) in the absence of extracellular Mg^{2+} triggered delayed, slow inward currents (SICs; Figure 1A). In three of these neurons, SICs were repetitively evoked by successive stimulations. The SICs occurred at low frequency (Figure 1B), and 12 of 14 events were recorded within the first minute after turning off the stimulation (mean delay ± SEM, 40.1 ± 8.2 s; n = 14). Compared to the excitatory postsynaptic current (EPSC), SICs displayed a notably slower rise time (92.3 ± 29.0 ms, n = 14 versus 6.4 ± 0.6 ms, n = 44), a decay fit by a single exponential function with a mean τ_{decay} = 568.5 ± 176.4 ms (EPSC

*Correspondence: gcarmi@bio.unipd.it
[3]These authors contributed equally to this work

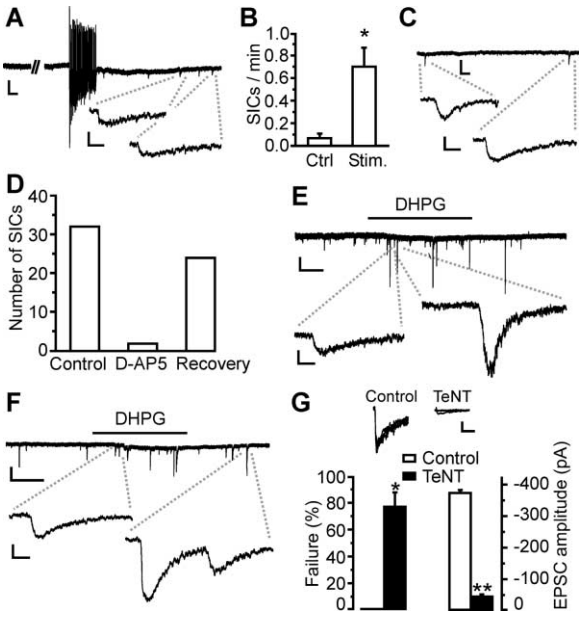

Figure 1. Slow Inward Currents Mediated Exclusively by NMDA Receptors Can Be Recorded from CA1 Pyramidal Neurons

(A) Representative whole-cell patch-clamp recording from a neuron after episodes of high-frequency SC stimulation. Three successive episodes of stimulation of 20 s duration were applied. While the first trial failed to trigger SICs, the second (shown in the figure) and the third trial evoked four and two SICs, respectively (some of these currents are shown at an expanded time scale). Scale bars, 100 pA and 10 s (top); 50 pA and 200 ms (bottom).

(B) Average number of SICs/min in six responsive neurons before and after SC stimulation. *$p < 0.05$.

(C) Examples of spontaneous SICs from a different neuron. Scale bars, 100 pA and 10 s; 50 pA and 200 ms.

(D) Total number of spontaneous SICs recorded under control conditions, in the presence of D-AP5 and after D-AP5 washout ($n = 2$).

(E) Recordings from a pyramidal neuron showing SICs triggered by 3 min application of 15 μM DHPG (thick line) in 1 μM TTX. Scale bars, 100 pA and 50 s; 50 pA and 200 ms. The EPSCs evoked by SC stimulation to the same neuron which displays DHPG-induced SICs have the typical fast activation of synaptic currents (rise time, 4.4 ± 0.2 ms, $n = 51$).

(F) In a slice incubated in 2 μM TeNT and perfused with TTX, 10 μM DHPG triggers SICs. Scale bars, 100 pA and 50 s; 50 pA and 200 ms.

(G) Average percentage of failures and EPSC amplitude in controls and in slices preincubated with TeNT. (Inset) Representative examples of four EPSCs recorded from neurons in a control slice (left) and in a TeNT-incubated slice (right). Scale bars, 100 pA and 100 ms. In this as well as the other figures, *$p < 0.05$, **$p < 0.001$.

$\tau_1 = 27.6 \pm 3.0$ ms, $\tau_2 = 146.1 \pm 12.0$ ms, $n = 44$), and a mean amplitude of -95.0 ± 36.7 pA (Supplemental Table S1 [http://www.neuron.org/cgi/content/full/43/5/729/DC1]). A fast AMPA component was always absent from the SIC.

SICs also occurred spontaneously (Figures 1B and 1C) at a very low frequency (number of SICs/min, 0.16 ± 0.04, $n = 65$; Supplemental Table S1 [http://www.neuron.org/cgi/content/full/43/5/729/DC1]), with the exception of three neurons (number of SICs/min, 3.1 ± 0.6). SICs are due to activation of NMDAR because they are reversibly blocked by 200 μM D-AP5, a specific NMDAR antagonist (Figure 1D).

In neurons of the ventrobasal thalamus, slice perfusion with *t*-ACPD (an agonist of mGluRs) triggered slow NMDAR-mediated inward currents (Parri et al., 2001) that were similar to the SICs reported here. In CA1 hippocampal neurons, slice perfusion with *t*-ACPD resulted in $[Ca^{2+}]_i$ elevations mediated by ionotropic GluR activation (Pasti et al., 1997). We thus asked whether mGluR stimulation with the group I mGluR agonist (S)-3,5-dihydroxyphenylglycine (DHPG; 10–30 μM) can trigger SICs in hippocampal neurons.

Patch-clamp recordings show that in a subpopulation of CA1 pyramidal neurons (27 of 98, 28%) DHPG triggered D-AP5-sensitive SICs that were indistinguishable from the SICs evoked by SC stimulation (Figure 1E; Supplemental Table S1 [http://www.neuron.org/cgi/content/full/43/5/729/DC1]). In the presence of (5*S*,10*R*)-(+)-5-Methyl-10,11-dihydro-5H-dibenzo[a,d]cyclohepten-5,10-imine maleate (MK-801, 20 μM), an open channel NMDAR blocker, a few SICs could be observed upon the first but not the second DHPG stimulation ($n = 4$). SICs reverse polarity at positive potentials (Supplemental Figures S1A and S1B) and are superimposed on a steady-state inward current mediated by activation of neuronal mGluR1 receptors (Congar et al., 1997; Crépel et al., 1994) (Supplemental Figure S2). SICs were observed with unchanged amplitude and kinetics in 6-nitro-7-sulphamoylbenzo[f]quinoxaline-2,3-dione (NBQX) (30 μM), a specific AMPAR antagonist (Supplemental Figures S1C and S1D). Desensitization of the AMPAR accounts for the absence of an AMPA component in SICs because, in the presence of D-AP5 and TTX, cyclothiazide, which reduces AMPAR desensitization (Yamada and Tang, 1993), unmasked DHPG-evoked inward currents that were abolished by NBQX (30 μM; Supplemental Figure S3).

The percentage of neurons displaying SICs upon DHPG stimulation and the frequency of SICs do not change significantly during the second (30%, n= 66; SICs/min, 1.2 ± 0.2; $n = 20$) or the third (24%, $n = 29$, SICs/min, 1.8 ± 0.7; $n = 7$) postnatal week. SICs were detected from all the three cells recorded in slices obtained from rats older than 21 days (data not shown).

Because experiments were performed in 1 μM tetrodotoxin (TTX) to block action potential generation, we suggest that SICs arise from a nonneuronal origin. In support of this notion, DHPG-evoked D-AP5-sensitive SICs were still present after slice incubation (2 hr) with 2 μM tetanus neurotoxin (TeNT), which blocks the synaptic release of neurotransmitters (Schiavo et al., 1992) (Figure 1F). Although we increased the stimulus intensity applied to SCs at least 10-fold in TeNT-incubated slices compared to controls, synaptic transmission was drastically impaired. In controls, each stimulus evoked an EPSC, while in TeNT the stimulus often failed to evoke an EPSC (Figure 1G, left), and the amplitude of the few responses that were observed was drastically reduced (Figure 1G, right and inset). Thus, SICs are due to NMDA receptor activation by glutamate of nonsynaptic origin.

Nonsynaptic Origin of Glutamate that Evokes SICs

Since $[Ca^{2+}]_i$ elevations trigger glutamate release from astrocytes (Bezzi et al., 1998; Parpura et al., 1994; Pasti et al., 2001) and SC stimulation (Pasti et al., 1997; Porter and McCarthy, 1996) evokes $[Ca^{2+}]_i$ elevations in astro-

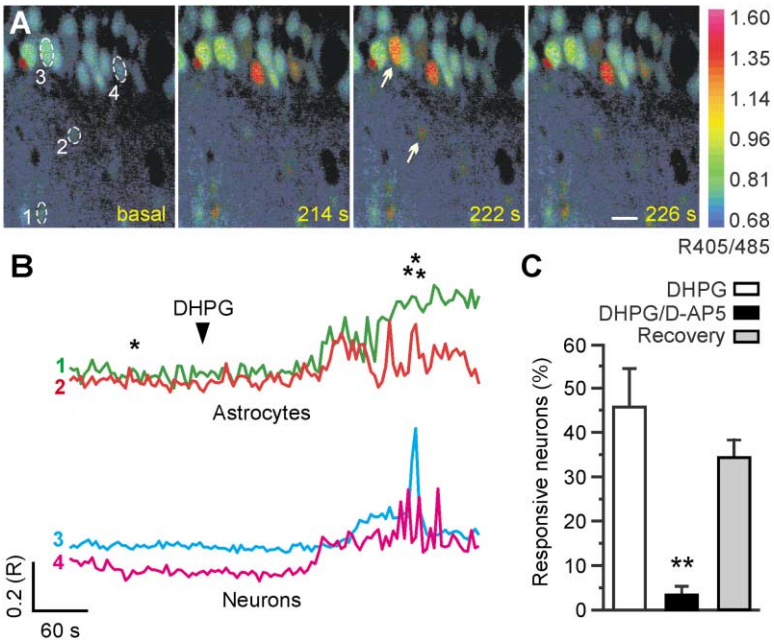

Figure 2. DHPG Triggers $[Ca^{2+}]_i$ Oscillations in Astrocytes and NMDAR-Mediated Ca^{2+} Responses in CA1 Pyramidal Neurons

(A) Sequence of pseudocolor images showing the $[Ca^{2+}]_i$ changes of two astrocytes (spots 1 and 2) and two pyramidal neurons (spots 3 and 4) after stimulation with 10 μM DHPG. In each frame, the timing after the onset of DHPG application is indicated. Sampling rate, 4 s. Scale bar, 20 μm. The ratio (R) of the intensity of the light emitted by Indo-1 at the two wavelengths (405/485) is displayed as a pseudocolor scale. Arrows indicate the $[Ca^{2+}]_i$ increases in astrocyte 2 and neuron 3.

(B) Time course of the 405/485 changes from astrocytes and neurons marked in (A). To better distinguish the response from each cell, in this as well as the other figures, some of the traces are shifted on the y axis. Basal 405/485 values in astrocytes and neurons were similar and ranged from 0.63 to 0.71. Asterisks mark the timing for the images shown in (A).

(C) Average percentage of DHPG-responsive neurons before D-AP5 application (n = 7), in the presence of D-AP5 (n = 7) and after its washout (n = 3).

cytes and nonsynaptic, glutamate-mediated SICs in pyramidal neurons, astrocytes are good candidates for a nonsynaptic source of glutamate.

To study the response of astrocytes to DHPG, we performed Ca^{2+} imaging experiments. In 1 μM TTX, DHPG triggered $[Ca^{2+}]_i$ elevations in the majority of astrocytes (mean ± SEM, 71.1% ± 9.2%, n = 14) and in a subpopulation of CA1 neurons (38.4% ± 5.5%, n = 14, Figures 2A and 2B; Supplemental Movie 1A [http://www.neuron.org/cgi/content/full/43/5/729/DC1]). Neuronal but not astrocytic $[Ca^{2+}]_i$ responses were reversibly blocked when DHPG was applied in 200 μM D-AP5 (Supplemental Movie 1B; Figure 2C). NBQX (10–50 μM; n = 2) and incubation with 2 μM TeNT did not block the action of DHPG (data not shown).

The results indicate that both SICs and transient $[Ca^{2+}]_i$ changes in pyramidal neurons reflect the same event, i.e., NMDAR activation by DHPG-induced glutamate release from a nonsynaptic origin, presumably astrocytes.

Other stimuli that are effective in evoking $[Ca^{2+}]_i$ oscillations in astrocytes, such as purinergic receptor agonists (Arcuino et al., 2002) and low Ca^{2+} (Parri et al., 2001; Zanotti and Charles, 1997), also evoke SICs (Supplemental Figure S4 [http://www.neuron.org/cgi/content/full/43/5/729/DC1]). The amplitude and kinetics of SICs evoked by the various stimuli are similar (Supplemental Table S1 and Supplemental Figure S4).

Stimulation of Individual Astrocytes Evokes SICs in Adjacent Neurons

To test the causal link between $[Ca^{2+}]_i$ increases in astrocytes and the NMDAR-mediated response in neurons, we used photolysis to evoke an $[Ca^{2+}]_i$ rise in single astrocytes while measuring SICs in a CA1 pyramidal neuron. Slices were loaded with the Ca^{2+} indicator fluo-4 AM and the Ca^{2+} cage NP-EGTA AM, which selectively loads into astrocytes but not into neurons (Sul et al., 2004). UV photolytic elevation of astrocytic Ca^{2+} evoked a SIC in the associated pyramidal neuron in 36% of the examples tested (n = 98; Figure 3). Photo release of Ca^{2+} in the astrocytic cell body locally elevates $[Ca^{2+}]_i$, which slowly propagates throughout the processes (Ca^{2+} wavefront velocity 1.05 ± 0.17 μm/s; n = 13). In each of four preparations where the dye-loaded dendrite and the astrocyte cell body were in the same focal plane, the Ca^{2+} wavefront reached the dendrite at the same time that the SIC was detected in the pyramidal neuron. Photolysis-induced SICs were of similar amplitude and kinetics (Supplemental Table S1 [http://www.neuron.org/cgi/content/full/43/5/729/DC1]; latency 12.2 ± 1.25 s) to those evoked by other stimuli which trigger $[Ca^{2+}]_i$ elevations in astrocytes. UV photolysis neither evoked a calcium elevation in the stimulated astrocyte nor a SIC in the associated pyramidal neuron (n = 8) when NP-EGTA was omitted.

To control for inadvertent stimulation of neuronal processes, we repositioned our photolysis beam to directly stimulate the neuronal dendrite. In this configuration, photolysis fails to evoke a neuronal SIC (n = 8), demonstrating that the calcium wavefront within the astrocyte is necessary for the generation of the neuronal SIC.

Using pairs of stimuli, we compared the relative SIC amplitudes in the presence and absence of NMDAR antagonists. In control conditions (0 Mg^{2+} saline), the SIC evoked by the second stimulus (P2) was similar in amplitude to the response evoked by the first (P1). In contrast, the addition of D-AP5 (50 μM) or 1 mM Mg^{2+} significantly depressed the SIC amplitude with no effect on the astrocytic $[Ca^{2+}]_i$ elevation (Figures 3B and 3C).

If the SIC is due to the astrocyte, repetitive stimulation of the same cell should evoke neuronal responses with a similar latency. Figure 3D shows that the stimulus-response latency for pairs of photolysis pulses was separated by 2 min; the first photolysis stimulus (P1) does predict the SIC latency following the second photostim-

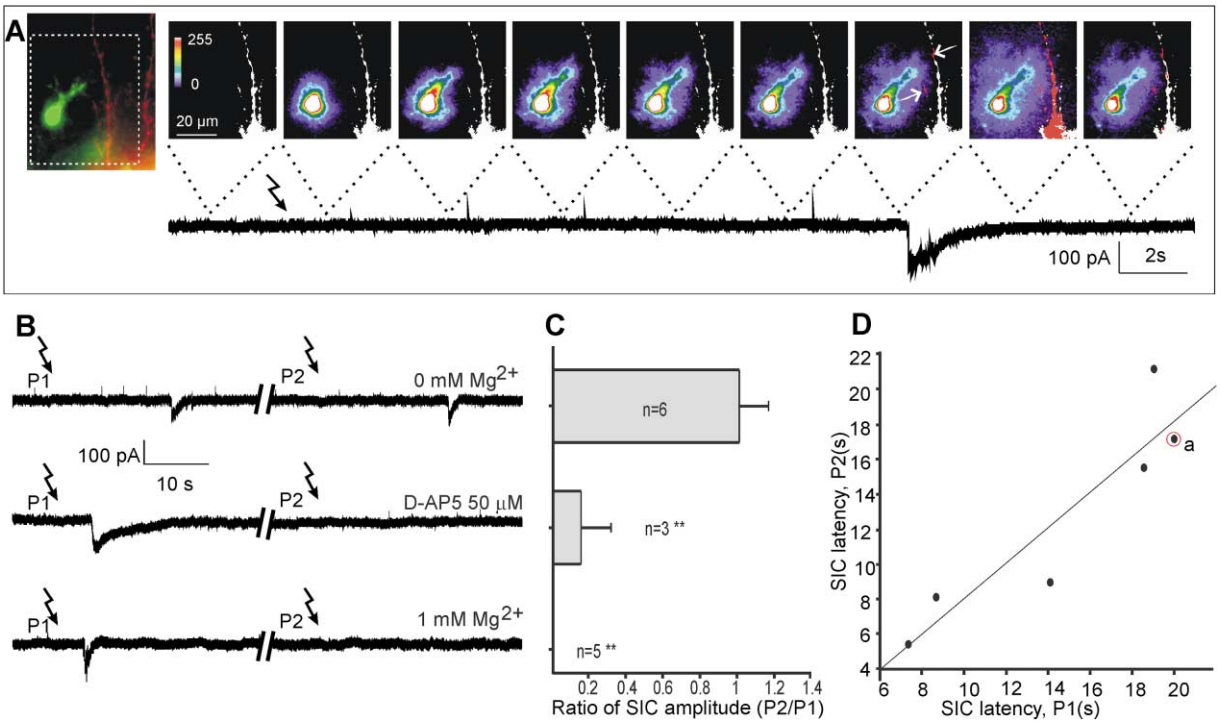

Figure 3. Photolytic Elevation of $[Ca^{2+}]_i$ in a Single Astrocyte Elicits an NMDA Receptor-Dependent SIC in an Adjacent Pyramidal Neuron

(A) Left image shows a fluo-4 and NP-EGTA-loaded astrocyte (green) adjacent to dendrites of an Alexa 568-filled CA1 pyramidal neuron (red). Subsequent images display percent changes in fluo-4 intensity in pseudocolor with an overlay image (white) showing the location of the pyramidal neuron dendrite. Images were taken at the times indicated by the dashed lines in the simultaneous current recording from the neuron (lower trace). Delivery of a UV pulse, between image 1 and 2, elevates $[Ca^{2+}]_i$ in the astrocyte cell body which slowly spreads through the astrocyte processes. By the seventh image in the sequence, changes in astrocyte fluorescence were detected in the same pixels as occupied by the neuronal dendrite (red pixels, arrows) that coincided with the onset of the SIC recorded in the neuron (lower trace).

(B) Pairs of photolysis pulses (P1 and P2) evoke similar amplitude SICs (top trace; 0 mM Mg^{2+}). Application of D-AP5 (50 μM; $p < 0.01$) or 1 mM Mg^{2+} ($p < 0.01$) 5 min before P2 significantly reduced the SIC amplitude.

(C) Histograms showing the average (±SEM) ratio of SIC amplitude (P2/P1) from experiments discussed in (B).

(D) The latencies of SICs following P1 predict the SIC latency in response to P2 ($r = 0.92$ $p < 0.01$). The point labeled in red represents the example shown in (A).

ulus (P2), supporting our contention that the SIC is evoked by the calcium elevation in the astrocyte.

Together with the results obtained in response to the other stimuli which mobilize astrocytic Ca^{2+} and evoke SICs, these data demonstrate a causal link between astrocytic $[Ca^{2+}]_i$ elevations and pyramidal neuronal SICs and show that this current is mediated largely by NMDAR activation.

Reverse Operation of Glutamate Transporters Does Not Mediate SICs

To determine whether glutamate is released through a reversal operation of glutamate transporters, experiments were performed in the presence of the glutamate transporter inhibitor DL-threo-β-benzyloxyaspartate (TBOA) (Shimamoto et al., 1998). The increase in the extracellular concentration of glutamate that follows TBOA application generated a D-AP5-sensitive inward current (-109.1 ± 20.3 pA; $n = 15$; Figure 4A). Under these conditions, astrocyte stimulation with DHPG still evoked SICs in 4 of 14 pyramidal neurons (29%) that were reversibly blocked by D-AP5 (Figures 4A and 4B). The mean decay time of SICs was 3-fold slower than in controls, while both mean rise time and amplitude were not significantly changed (Figures 4C and 4D). The slower decay time is consistent with the delayed clearance of glutamate in the extracellular space.

Extrasynaptic NMDARs Mediate SICs

The slow decay time of ~90% of SICs (Supplemental Figure S4E [http://www.neuron.org/cgi/content/full/43/5/729/DC1]) suggests that the NMDAR mediating SICs is composed mainly of the NR1/NR2B complex, which is characterized by slow offset kinetics (Dingledine et al., 1999). To test the hypothesis that astrocytic glutamate acts preferentially on the NR1/NR2B complex, we used the selective NR2B antagonist ifenprodil (10 μM), which blocks 80% of the current mediated by the NR1/NR2B complex (Williams, 1993). In the presence of 5–10 μM ifenprodil, the SIC amplitude was drastically and reversibly reduced (Figure 4E), while the NMDA-mediated EPSCs evoked by SC stimulation were affected only slightly (Figures 4F and 4G).

Glutamate Released from Astrocytes Triggers Synchronized Responses in Multiple Neurons

We frequently observed simultaneous transient $[Ca^{2+}]_i$ increases in several CA1 neurons following astrocytic

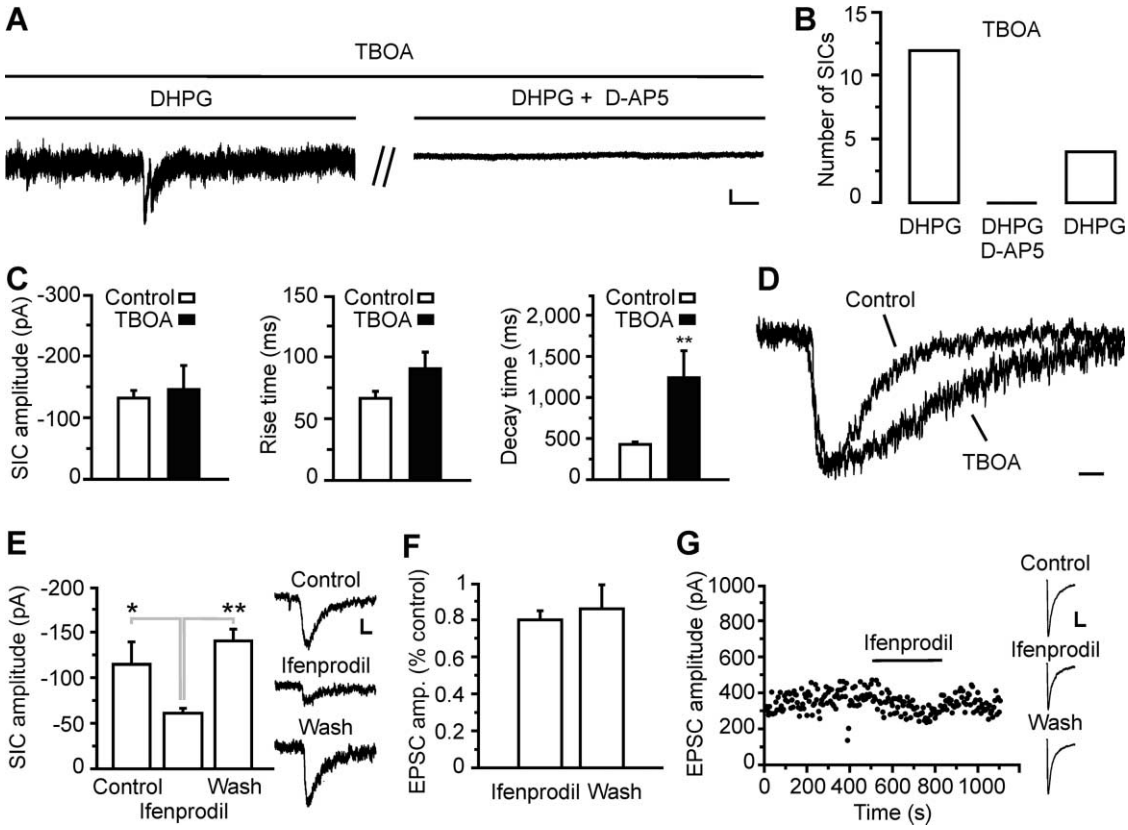

Figure 4. SICs Are Not Inhibited by the Glutamate Transporter Antagonist TBOA and Are Mediated Mainly by the Activation of NR1/NR2B Complex

(A) In the presence of 100 μM TBOA, 10 μM DHPG still triggers SICs (left). In the same neuron, in the presence of D-AP5, a successive stimulation with DHPG fails to evoke SICs (right). In the presence of TBOA, DHPG evoked SICs in 4 of 10 (40%) cells, with a mean frequency of 1.3 ± 0.3 SICs/min. Scale bars, 50 pA and 5 s.

(B) Total number of SICs in the four responsive neurons in the presence of TBOA (50–100 μM), TBOA plus D-AP5, and after TBOA washout.

(C) Average amplitude (n = 17) and rise (n = 15) and decay (n = 17) time of SICs in the presence of TBOA. As a control, we reported the average value of amplitude (n = 259) and rise and decay time (n = 202) of SICs recorded in in the absence of TBOA.

(D) Examples of normalized SICs under control conditions and in the presence of 100 μM TBOA. Scale bar, 200 ms.

(E) Mean amplitude of DHPG- and low Ca^{2+}-induced SICs in control condition (n = 21, 2 cells), in the presence of 5–10 μM ifenprodil (n = 57; 5 cells) and after its washout (n = 45, 5 cells). The inset shows representative examples of SICs under the different experimental conditions. Scale bars, 50 pA and 200 ms.

(F) In four cells, including one of the cells included in (E), 10 μM ifenprodil slightly but not significantly reduces the peak amplitude of NMDA EPSCs. All EPSCs are recorded in the presence of 30 μM NBQX.

(G) Representative experiment showing the time course of the NMDA EPSC amplitude at basal conditions, during 10 μM ifenprodil application and after its washout. The inset shows averages of 20 EPSCs in the different experimental conditions. Scale bars, 100 pA and 200 ms.

stimulation. In Figures 5A and 5B (also see Supplemental Movie 2 [http://www.neuron.org/cgi/content/full/43/5/729/DC1]), the $[Ca^{2+}]_i$ elevation in a stratum radiatum astrocyte is followed by an $[Ca^{2+}]_i$ increase in three adjacent pyramidal neurons. This increase is short lasting (2 s) and occurs synchronously in the three neurons (Figure 5B). Paired recordings made from pyramidal neurons while stimulating glutamate release from astrocytes with either DHPG or low Ca^{2+} in TTX demonstrated that SICs can occur in the two neurons with a high degree of temporal correlation. Figure 5C shows that only a few milliseconds separate the onset of synchronous SICs that occur in two neurons spontaneously as well as following DHPG stimulation. Note that the two subsequent SICs that occur in the first neuron are accompanied by only one synchronized event in the second neuron. Synchronized SICs are always characterized by the typical slow kinetics of SICs. Depolarizing voltage pulses applied to each neuron of the pair revealed no evidence of electrical coupling (Figure 5D; n = 8). At least two synchronized events were detected in 10 of 25 pair recordings. The interevent time interval histogram of SICs from a total of ten pairs demonstrates that 23% of SICs (44 of 195) were synchronized within a time window of 100 ms (Figure 5E). Such a level of coincidence did not arise randomly among events from paired recordings. Indeed, predictions obtained by a Monte Carlo simulation or by an analysis of the Poisson distribution demonstrate that in a 100 ms time window the probability of detecting a pair of coincident events is less than 0.001 and that to attain by chance the level of SICs coincidence that we observed in our paired recordings would require a time window of 30 s (Figure 5F).

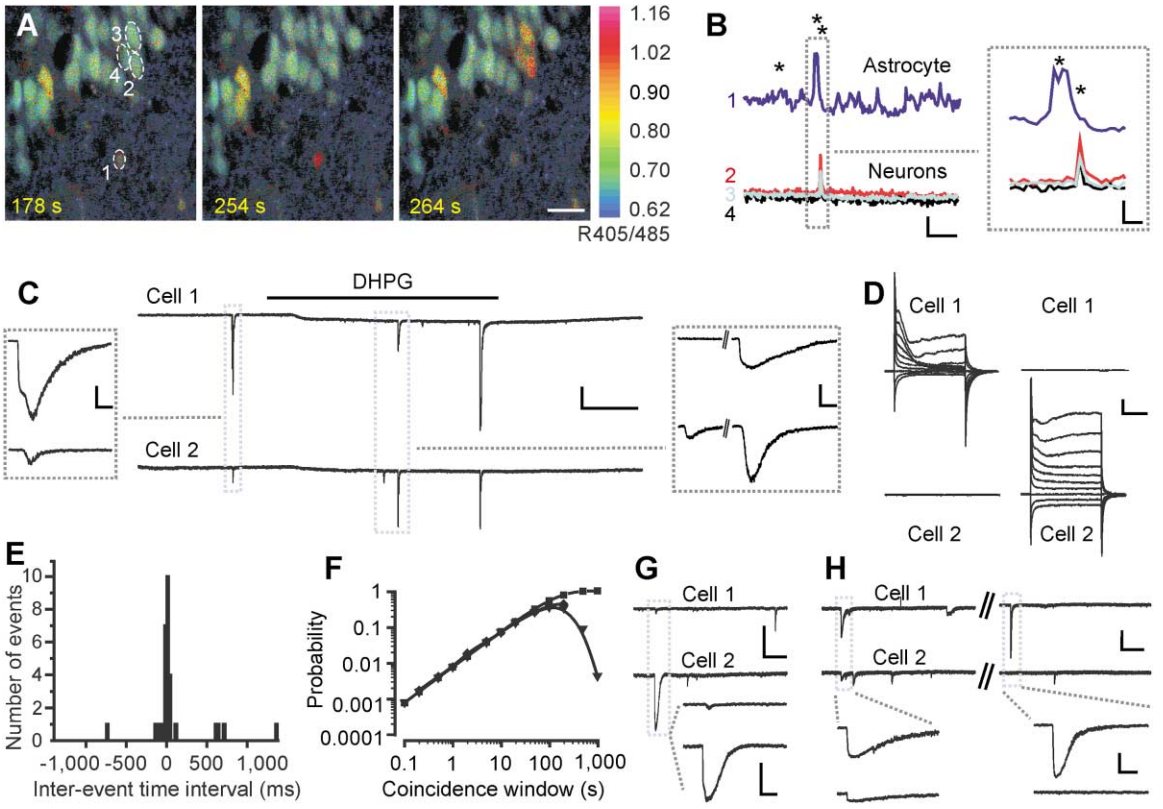

Figure 5. SICs from Distinct Neurons Can Occur with a High Degree of Synchronization

(A) $[Ca^{2+}]_i$ changes occurring in one astrocyte (1) and three neurons (2, 3, and 4) upon low Ca^{2+} stimulation. Sampling rate, 2 s. Scale bar, 20 μm.

(B) Time course of the response from the same cells indicated in (A). Scale bars, 0.1 (R), 60 s. Note that the Ca^{2+} elevation in astrocyte 1 precedes the synchronous response in neurons 2, 3, and 4 (right). Scale bars, 0.1 (R), 8 s.

(C) Patch-clamp, paired recordings from two CA1 pyramidal neurons showing synchronized SICs after 20 μM DHPG stimulation in 1 μM TTX. Scale bars, 200 pA and 50 s; inset 200 pA and 400 ms. The somata of the two neurons are 30 μm apart.

(D) Same pair of neurons as in (C), showing that voltage steps (from −80 to +10 mV) applied to each cell do not propagate to the other cell of the pair. Traces are not leak subtracted. Scale bars, 250 pA and 40 ms.

(E) Interevent time interval histogram of SICs occurring in the two neurons from ten pairs. A total number of 39 time intervals were counted in a window of ±6 s. The majority of these (31/39) are restricted to a time window of ±1.5 s (shown in the figure). Note that 44 SICs, i.e., 22 of these time intervals, are restricted within a time window of 100 ms. Bin, 25 ms. The mean frequency of SICs in neurons from pair recordings is 0.45 ± 0.08 events/min.

(F) Probability of observing coincident events according to a Monte Carlo simulation or analysis of the Poisson distribution. With a time window of 100 ms and a frequency of events of 0.45 events/min, the probability of detecting a pair of coincident events is less than 0.001. Monte Carlo simulation (◆); probability of 1 or more coincidences (■); probability of exactly 1 coincidence (▼).

(G) Paired recording showing a large-amplitude SIC in neuron 2 and a synchronized, small-amplitude SIC in neuron 1 triggered by 10 μM DHPG stimulation. Scale bars, 200 pA and 10 s; 200 pA and 2 s.

(H) Paired recording from two neurons showing spontaneous, synchronous SICs. Scale bars, 200 pA and 10 s; 200 pA and 400 ms. The distance between the somata of the neurons from the pairs shown in (G) and (H) is 100 μm.

The synchronized SICs could have very different amplitudes (Figures 5G and 5H), and large-amplitude events detected in one neuron were not always accompanied by a synchronized event from the other neuron of the pair (Figure 5H, right).

Neuronal somata separated by up to 100 μm could exhibit synchronized SICs. This suggests that glutamate release from astrocytes acts simultaneously on more than two neurons. We thus performed additional confocal imaging studies with relatively high temporal resolution (1 or 2 s). Slices were perfused with 1 μM TTX and astrocytes were stimulated with low Ca^{2+}, DHPG, or (RS)-2-chloro-5-hydroxyphenylglycine (CHPG), a specific agonist of the mGluR5 subtype. This compound efficiently evoked $[Ca^{2+}]_i$ oscillations in astrocytes as well as $[Ca^{2+}]_i$ elevations (Figure 6) and SICs in neurons (see Supplemental Figure S2D [http://www.neuron.org/cgi/content/full/43/5/729/DC1]). In Figures 6A and $6A_1$ (see also Supplemental Movie 3), following low Ca^{2+} stimulation, groups of neurons displayed three successive, short-lasting, synchronous $[Ca^{2+}]_i$ responses. Several neurons participated in the three responses, and in the second episode, a domain of nine neurons displayed a synchronous $[Ca^{2+}]_i$ elevation of one frame duration, i.e., equal to or less than 2 s (Figure $6A_1$; see also Supplemental Movie 3). Repetitive responses from the same neurons were frequently observed. In the example illustrated in Figures 6B and 6C, astrocyte stimulation with 1 mM CHPG first triggered in four neurons a synchronous response (Figures 6B and $6B_1$) and then a short-

lasting $[Ca^{2+}]_i$ elevation restricted to a dendrite together with a synchronous $[Ca^{2+}]_i$ elevation at the somata of two other neurons (Figures 6C and $6C_1$; Supplemental Movie 4). In all neurons from all experiments, synchronous responses were abolished by D-AP5. The interevent time interval histogram of the neuronal response from the experiment illustrated in Figures 6B and 6C reveals that the large majority of $[Ca^{2+}]_i$ elevations from each neuron occurred in the same time frame with at least one $[Ca^{2+}]_i$ elevation from another neuron in the field (Figure 6D). Only 22% (25 of 113) of the responses occurred in solitary neurons. The majority of the responses in the astrocytes (65 of 72, 90%) were coincident with or preceded those in neurons (Figure 6E). Results from a total of 22 experiments reveal that the majority of domains are composed of two to four contiguous neurons, although domains comprising a higher number of neurons are also present (Figure 6F). Figure 6G reports the maximal spatial extent of the domain expressed as a function of the number of neurons in the domain. Besides the expected positive correlation between these two values, the graph reveals that two or three noncontiguous neurons located up to a distance of approximately 100 μm can display synchronized responses.

In one additional experiment in which a time acquisition of 1 s was applied, 98 of 143 (69%) $[Ca^{2+}]_i$ elevations in neurons occurred synchronously upon astrocyte stimulation. From a total of four experiments with a time resolution of 1 or 2 s, 70% $\pm$ 6% of $[Ca^{2+}]_i$ elevations from an individual neuron occurred within a time window of 2 s with at least one other neuron in the field of view.

Synaptic Activation of Astrocytes Evokes Feedback Neuronal Synchronization

Since synaptic release of glutamate can trigger $[Ca^{2+}]_i$ oscillations in astrocytes (Pasti et al., 1997; Porter and McCarthy, 1996), we asked whether activated astrocytes can signal back to neurons and trigger NMDAR-dependent synchronized responses in neuronal domains. This series of experiments (n = 4) was performed at physiological temperature (35°C) and in the absence of Mg^{2+} and picrotoxin. Application of short stimulus trains (see Experimental Procedures) to SCs evoked in CA1 pyramidal neurons $[Ca^{2+}]_i$ elevations in response to each applied stimulus (Figures $6H_2$ and 6I) and a delayed $[Ca^{2+}]_i$ elevation in astrocytes (cells 5, 6, and 7; Figures $6H_3$ and 6I). Turning off the stimulation while applying TTX caused the neuron responses to cease immediately. In contrast, $[Ca^{2+}]_i$ oscillations in the astrocytes continued (Figure 6I). Our prediction was that these $[Ca^{2+}]_i$ oscillations could mediate the release of glutamate from these cells and activate synchronized responses in pyramidal neurons. In the example reported, a synchronous $[Ca^{2+}]_i$ elevation in a neuronal domain that involved three neurons is illustrated (Figures $6H_4$ and 6I). One of these neurons displayed a second response in synchrony with a contiguous neuron that was not involved in the first response. The interevent time interval histogram from this experiment reveals that the majority of $[Ca^{2+}]_i$ elevations (22 of 30, 73%) from each neuron occurred in the same time frame (time acquisition, 1 s) with at least one $[Ca^{2+}]_i$ elevation from another neuron in the field (Supplemental Figure S5A [http://www.neuron.org/cgi/content/full/43/5/729/DC1]). The majority of the responses in the astrocytes (31 of 39, 75.5%) were coincident with or preceded that in neurons (Supplemental Figure S5B). As expected, the domain response was reversibly inhibited by D-AP5 (Supplemental Figures S5C and S5D). The great majority of domains are composed of two to four neurons (mean, 2.56 $\pm$ 0.02), although domains comprising a higher number of neurons are also present (Supplemental Figure S5E). As a whole, we observed delayed responses in 47 of 133 neurons (35% $\pm$ 6%; n = 4), and 59% $\pm$ 9% of these responses from individual neurons occurred in synchrony with at least one other neuron in the field of view. The mean amplitude and frequency of $[Ca^{2+}]_i$ elevations in these responsive neurons was 0.16 $\pm$ 0.02 (R405/485 change) and 1.3 $\pm$ 0.47 events/min, respectively. SC stimulation triggered long-lasting $[Ca^{2+}]_i$ oscillations in 21 of 46 astrocytes (48% $\pm$ 12%, n = 4).

Astrocyte-Mediated Neuronal Synchrony under Physiological Conditions

We next investigated whether the domain response could be triggered by astrocytic glutamate in physiological conditions at 35°C in the presence of 1 mM extracellular Mg^{2+}, in the absence of picrotoxin, and in 1 μM TTX. Activation of astrocytes by either DHPG or PGE_2 evoked SICs (Figures 7A and 7B, respectively), although in a significantly lower percentage of neurons (10.7%, n = 56 versus 28%, n = 98, at 1 mM and 0 Mg^{2+}, respectively, Fisher's exact test, $p < 0.05$) and lower frequency (Figure 7C). Under these physiological conditions, the mean rise and decay times of SICs were unchanged, although their mean amplitude was significantly reduced (Figure 7D). SC stimulation in 1 mM Mg^{2+} also evoked SICs in 6 of 11 neurons (Figures 7E and 7F; Supplemental Table S2 [http://www.neuron.org/cgi/content/full/43/5/729/DC1]).

Similar to results obtained in the absence of Mg^{2+}, in 1 mM Mg^{2+} SICs can occur in pairs of neurons with a high degree of temporal correlation (Figures 7G and 7H). Depolarizing voltage pulses applied to each neuron of the pair revealed no evidence of electrical coupling (Figure 7G1; n = 3). In 7 of 13 pairs that displayed SICs, we detected at least two synchronized events. In these 7 pairs of neurons, we observed a total of 67 SICs, and 30% of these events were synchronized within a time window of 100 ms (Figure 7I). Given that, in the presence of Mg^{2+} astrocytic glutamate was still capable of eliciting synchronous SICs, we confirmed that astrocyte-mediated synchronization of neuronal domains could be similarly detected under these conditions. Stimulation of SCs in the presence of Mg^{2+} evoked long-lasting $[Ca^{2+}]_i$ oscillations in 23 of 35 astrocytes (62% $\pm$ 6%, n = 4) in a similar manner to when stimulation was performed in 0 Mg^{2+}. The sequence of images in Figure 8A shows the resulting $[Ca^{2+}]_i$ elevations that were evoked in CA1 pyramidal neurons by SC stimulation (Figure $8A_2$) and a delayed, synchronous $[Ca^{2+}]_i$ elevation in a domain that involved eight neurons (Figures $8A_4$ and 8B; Supplemental Movie 5 [http://www.neuron.org/cgi/content/full/43/5/729/DC1]). The large majority of $[Ca^{2+}]_i$ elevations (37 of 43, 86%) from each neuron occurred in the same time

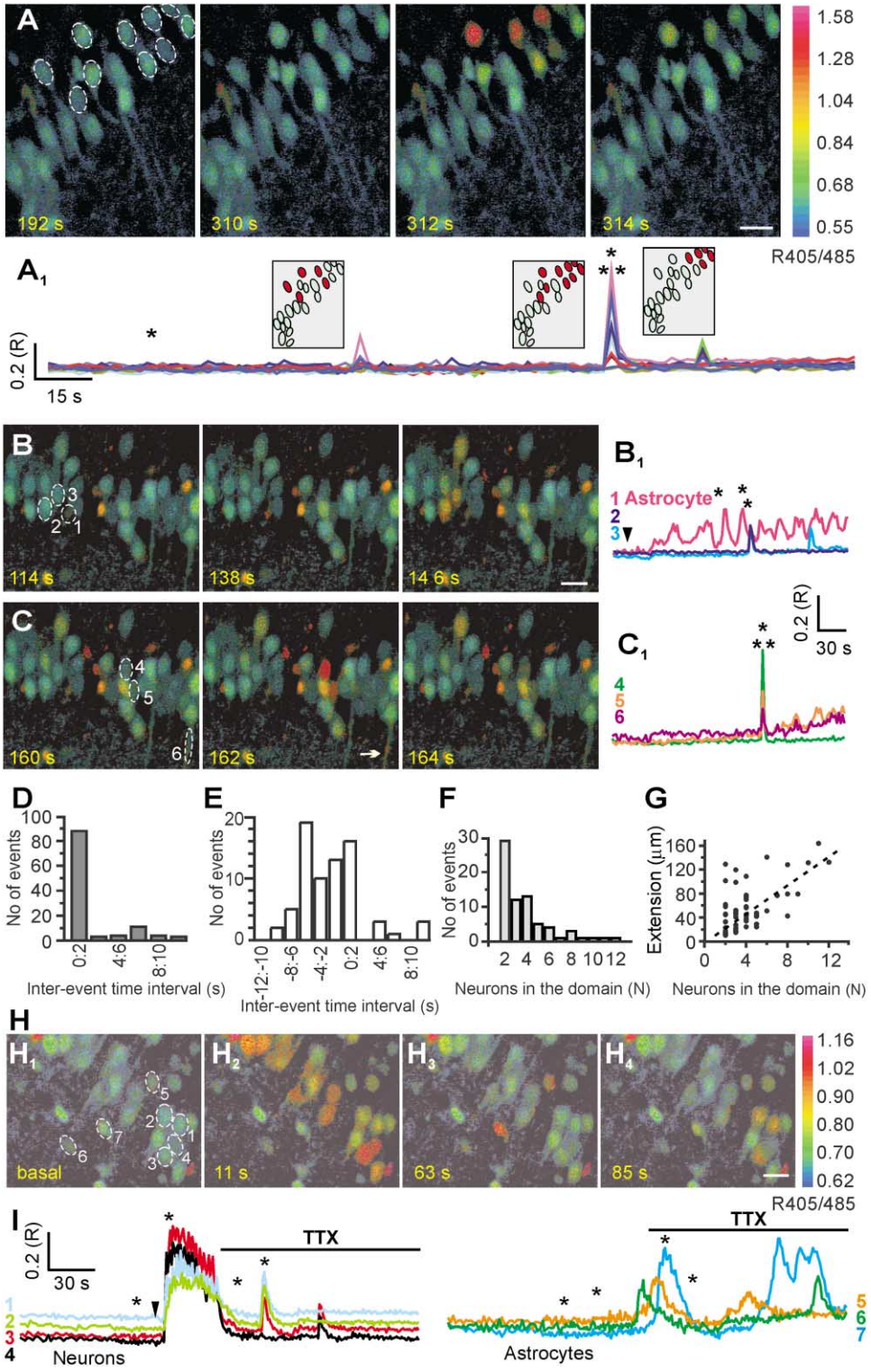

Figure 6. Astrocytic Glutamate Triggers Synchronized $[Ca^{2+}]_i$ Elevations in Neuronal Domains

(A) Low Ca^{2+} stimulation triggers synchronous $[Ca^{2+}]_i$ increases in nine pyramidal neurons in TTX. Sampling rate, 2 s. Scale bar, 20 μm.

(A_1) Time course of 405/485 changes for the neurons shown in (A). The inset marks the responsive neurons in the field (red) displaying synchronous responses.

(B) CHPG-induced $[Ca^{2+}]_i$ oscillations in one astrocyte (1) is followed by a synchronous response in four nearby neurons. Two of these are indicated (2 and 3). Sampling rate, 2 s. Scale bar, 20 μm. The time course of the 405/485 change from the astrocyte and two of the responsive neurons is reported in (B_1).

(C) Same field as in (B), illustrating the synchronous response from the soma of two neurons (4 and 5) and the dendrite of a third neuron (6) to CHPG stimulation. Sampling rate, 2 s. Scale bar, 20 μm. The time course of the 405/485 change for the dendrite and two other neurons is shown in (C_1).

frame (time acquisition, 1 s) with at least one $[Ca^{2+}]_i$ elevation from another neuron in the field (Figure 8C). In comparison to conditions that favor the activation of the NMDA receptor, these events were observed in a reduced percentage of neurons (19 of 156, 12% ± 5%; $n = 5$; $p < 0.05$) and at a lower frequency (0.48 ± 0.08 events/min; $p < 0.05$), while their mean amplitude (405/408 change, 0.19 ± 0.04) was not significantly changed. The distribution of the number of neurons composing the domain (Figure 8D) as well as the mean number of neurons in the domains (3.7 ± 0.1) are also similar. From four experiments with a time resolution of 1 s, 72% ± 10% ($n = 176$) of $[Ca^{2+}]_i$ elevations from an individual neuron occurred within a time window of 1 s with at least one other neuron. Thus, the presence of SICs and the synchronous activation of groups of neurons can be observed in more physiological conditions when GABAergic synaptic transmission is intact and Mg^{2+} is present in the external saline.

Discussion

Glutamate Released from Astrocytes Triggers Slow NMDAR Responses in CA1 Pyramidal Neurons

The inward currents generated by the activation of NMDARs described in our study are different from synaptic EPSCs because they have one order of magnitude slower rise times, never have an AMPA component, and are mediated mainly by the NR1/NR2B complex. Blockade of neuronal activity and synaptic transmission with TTX and TeNT allows us to rule out synaptic release from axon terminals as a source of the neurotransmitter, including asynchronous release that, in principle, may be responsible for the slow kinetics of SICs (Diamond and Jahr, 1995). Accordingly, the most likely source of this glutamate is from elements that are in proximity to the neuronal membrane, such as the astrocytic processes. This conclusion is supported by the observations that (1) stimuli that evoke $[Ca^{2+}]_i$ oscillations and glutamate release from astrocytes trigger NMDAR-mediated SICs and $[Ca^{2+}]_i$ elevations in CA1 pyramidal neurons; (2) stimulation of SCs, which evokes $[Ca^{2+}]_i$ oscillations in astrocytes (Pasti et al., 1997), also triggers SICs and $[Ca^{2+}]_i$ elevations in neuronal domains; (3) $[Ca^{2+}]_i$ elevations in activated astrocytes precede or are coincident with $[Ca^{2+}]_i$ elevations in pyramidal neurons; and (4) selective stimulation of $[Ca^{2+}]_i$ elevations in individual astrocytes—through flash photorelease of Ca^{2+}—triggers SICs in nearby neurons. This last observation provides conclusive evidence for a causal link between astrocyte $[Ca^{2+}]_i$ increase and the NMDA receptor-mediated response in neurons.

The slow rise and decay times that characterize SICs may be due to a slow glutamate release mechanism, the distance between the site of release and the target membrane receptors, as well as the coefficient of diffusion. We favor the possibility that these kinetics arise from a slow increase in glutamate concentration in the vicinity of the extrasynaptic neuronal receptors. Such a slow increase in glutamate concentration can also account for the absence of an AMPA component in SICs. Indeed, when AMPA receptor desensitization was reduced by addition of cyclothiazide, astrocyte activation evoked AMPA-mediated events with a slow rise time. This observation also indicates that glutamate and not aspartate is the principal mediator of SICs, since the latter does not activate the AMPA receptor (Patneau and Mayer, 1990).

The drastic reduction in SIC amplitude by the antagonist of the NR1/NR2B complex, ifenprodil, indicates that SICs are mediated mainly by the NR1/NR2B receptor. Indeed, after the second postnatal week, while the NR2A subunit dominates at the synapse, the NR2B subunit is confined mainly to the extrasynaptic membrane (Rumbaugh and Vicini, 1999; Tovar and Westbrook, 1999). Our results thus suggest that the release of glutamate from astrocytes into a relatively large extracellular space leads to a slow yet selective activation of extrasynaptic NMDARs.

The reverse operation of glutamate transporters (Attwell et al., 1993) is not involved in the generation of SICs, since they were still evoked in the presence of the transporter inhibitor TBOA. While astrocytes are known to release glutamate through various mechanisms (Haydon, 2001; Fellin and Carmignoto, 2004), a Ca^{2+}-dependent mechanism is involved in SIC generation. Indeed, all the stimuli that activate $[Ca^{2+}]_i$ elevations in astrocytes also trigger SICs and, most important, photolysis of caged Ca^{2+} in single astrocytes evokes SICs in nearby neurons. While further studies will be necessary for a full clarification of the cellular mechanism underlying glutamate release that generates SICs, our results are compatible with the recent demonstration that astrocytes possess a mechanism for a regulated, vesicular release of this transmitter (Bezzi et al., 2004).

Astrocytic glutamate-mediated responses were observed only in a subpopulation of neurons. While this may be due to the fact that the stimuli that we provided only activated a subpopulation of astrocytes, it is also important to appreciate that astrocytic processes are not uniformly distributed around the synapses (Ventura

(D) Interevent time interval histogram for the $[Ca^{2+}]_i$ elevations in neurons (bin, 2 s) in the experiment shown in (B)–(C).
(E) Interevent time interval histogram reporting the timing for the $[Ca^{2+}]_i$ elevation in each astrocytes with respect to the timing for the $[Ca^{2+}]_i$ elevation in neurons (bin, 2 s) in the same experiment shown in (B)–(C). The average time interval between the astrocytic and the neuronal response is 2.7 ± 0.5 s.
(F) Histogram of the number of responsive neurons in the domain after stimulation with either DHPG, CHPG, or low Ca^{2+} from 22 experiments.
(G) Maximal spatial extension of domains as a function of the number of neurons in the domain which display synchronous response to DHPG/CHPG or low Ca^{2+} stimulation.
(H) Pseudocolor images showing $[Ca^{2+}]_i$ elevations in neurons due to SC stimulation (H_2), delayed $[Ca^{2+}]_i$ elevations in astrocytes (H_3), and a synchronous response in three pyramidal neurons (H_4). Sampling rate, 1 s. Scale bar, 20 μm. These experiments were performed at 35°C in 1 μM TTX and in the absence of picrotoxin.
(I) Time course of 405/485 changes from the four neurons and the three astrocytes indicated in (H_1).

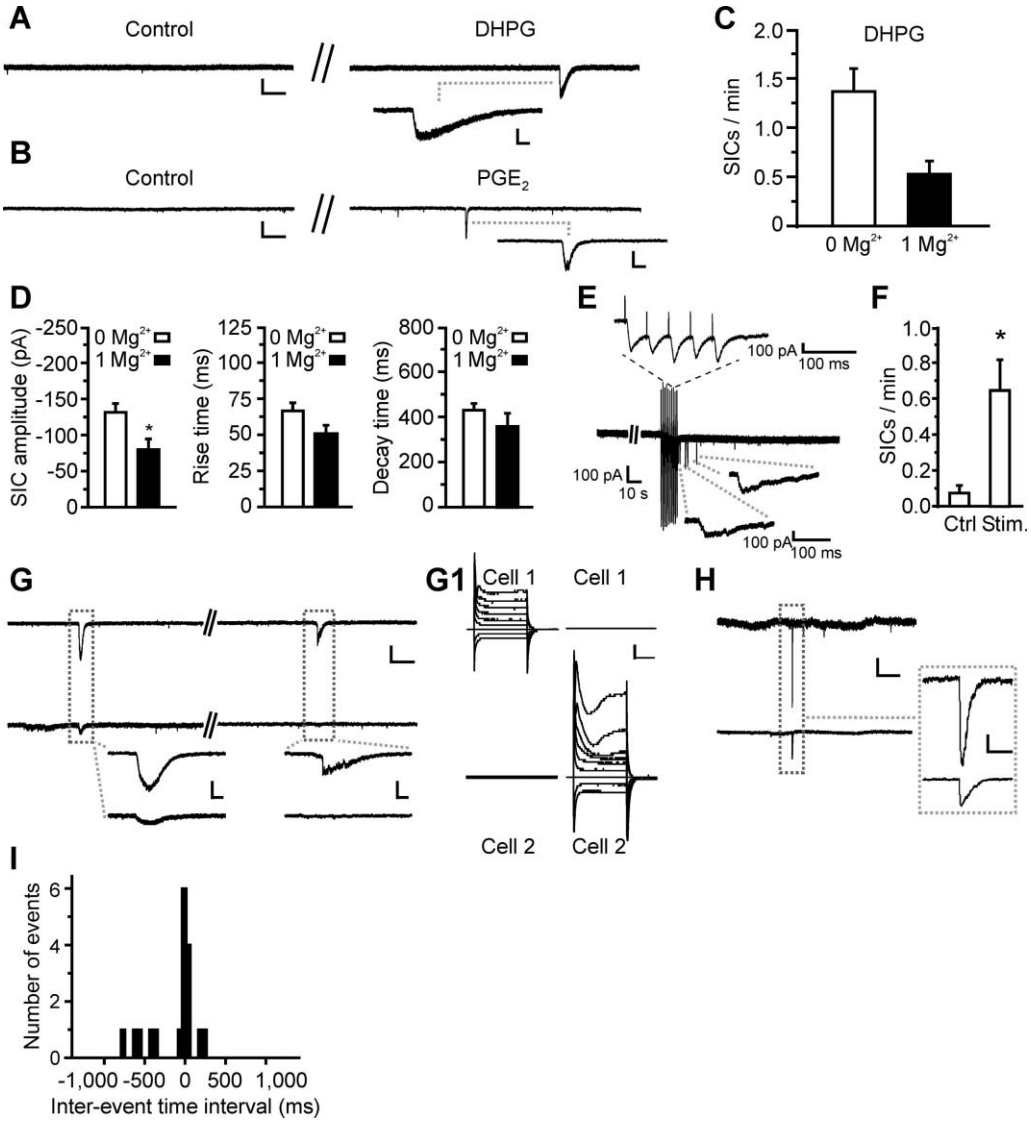

Figure 7. Astrocyte Activation in 1 mM Mg^{2+} Triggers Solitary as well as Synchronized SICs

(A) DHPG-evoked SIC at 35°C, 1 mM extracellular Mg^{2+}, in TTX and in the absence of picrotoxin. DHPG triggers SICs in 8 of 74 CA1 neurons. Scale bars, 50 pA and 5 s; 50 pA and 400 ms.

(B) SICs evoked by stimulation with 5 μM PGE_2, under the same experimental conditions as in (A). PGE_2 triggers SICs in 3 of 19 CA1 neurons. Scale bars, 50 pA and 5 s; 50 pA and 400 ms.

(C) Average number of SICs/min following DHPG stimulation in either 0 mM Mg^{2+} ($n = 27$) or in 1 mM Mg^{2+} ($n = 8$). The two values are not significantly different ($p = 0.06$).

(D) Average amplitude and rise and decay time for spontaneous and evoked SICs in 1 mM Mg^{2+} ($n = 83$). As a control, we reported the average value of amplitude ($n = 259$) and rise and decay time ($n = 202$) of spontaneous and evoked SICs recorded in 0 extracellular Mg^{2+}.

(E) Stimulation of SCs evokes SICs in 1 mM Mg^{2+} (bottom, individual SICs at expanded time scale; top, EPSCs triggered by a stimulus train).

(F) Average frequency of SICs before and following SC stimulation ($n = 6$).

(G) Synchronous (left) and solitary (right) SICs evoked by astrocyte stimulation with DHPG in 1 μM TTX. Scale bars, 50 pA and 5 s; 50 pA and 400 ms. The somata of the two neurons were 70 μm apart.

(G1) Same pair of neurons as in (G), showing the trace following voltage steps (from −80 to 0 mV) applied to each cell of the pair. Scale bars, 250 pA and 40 ms.

(H) An additional example of synchronous SICs evoked by astrocyte stimulation with DHPG. Note the relatively fast kinetics of these synchronous SICs. The somata of the two neurons were 10 μm apart. Scale bars, 50 pA and 5 s; 50 pA and 200 ms.

(I) Interevent time interval histogram of SICs occurring in the two neurons from seven distinct dual recordings. A total of 19 time intervals were counted in a window of ±6 s. The majority of these (18/19) are restricted to a time window of ±1.5 s (shown in the figure). Note that 20 SICs, i.e., 10 of these time intervals, are restricted within a time window of 100 ms. Bin, 50 ms. The mean frequency of SICs in neurons from pair recordings is 0.22 ± 0.07 events/min.

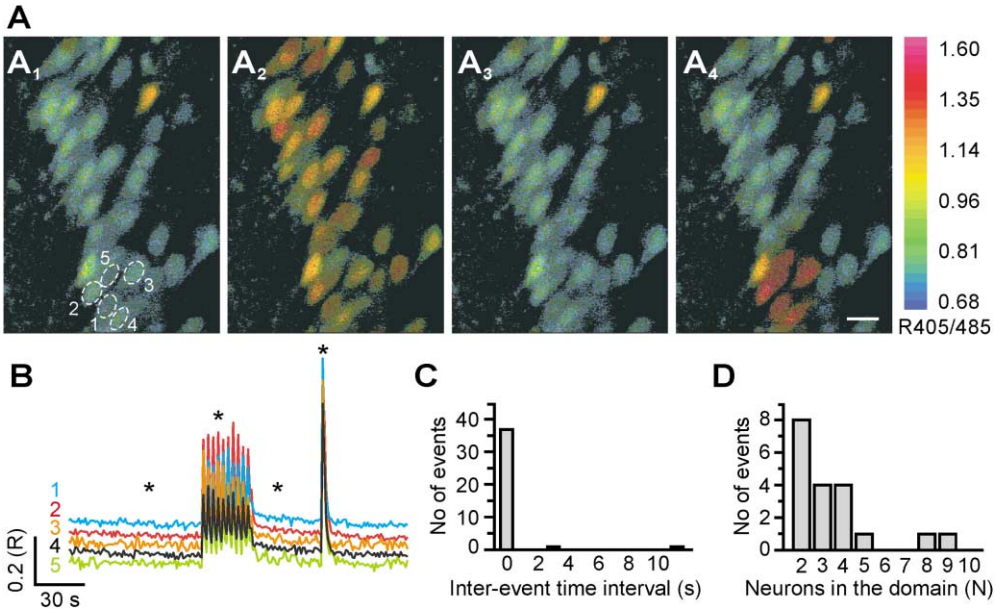

Figure 8. Neuronal Activity-Dependent Domain Responses under Physiological Conditions

(A) Images showing synchronous $[Ca^{2+}]_i$ elevations in neurons following stimulation of the SCs (A_2) and a synchronous delayed response from eight contiguous pyramidal neurons (A_4) under physiological conditions; scale bar, 20 μm. Note that no astrocytes could be visualized in this field at the same focal plane of responsive neurons.

(B) Time course of 405/485 changes from five of the neurons composing the domain.

(C) Interevent time interval histogram for the $[Ca^{2+}]_i$ elevations in neurons (bin, 1 s) from the same experiment.

(D) Histogram of the number of responsive neurons in the domain from five experiments.

and Harris, 1999) and that hippocampal astrocytes represent a heterogeneous population that may have different functional properties (Matthias et al., 2003).

Glutamate Released from Astrocytes Synchronizes Activity in Neuronal Domains

The synchronized activation of groups of neurons mediated by extrasynaptic NMDARs represents one of the main findings of this study. In paired recordings, we observed that SICs could occur in two neurons with a high degree of temporal correlation. Such a high synchronization cannot derive from spreading of the current through gap junctions, since we never detected signs of electrotonic coupling between neurons which display synchronized responses. Additionally, synchronized events cannot be due to activation of NMDARs by synaptically released glutamate because they are not affected by TTX, which blocks action potential discharges, they are too slow for synaptic mediated events, and because TeNT, which blocks synaptic release of glutamate, does not impair SICs. It is unlikely that the intercellular Ca^{2+} wave among multiple astrocytes mediates neuronal synchrony because this wave propagates at a speed of approximately 10 μm/s (Sul et al., 2004). The most likely explanation for synchronized events is that they are derived from a single episode of astrocytic glutamate release that activates extrasynaptic NMDARs from the adjacent dendrites of neurons that are close enough to simultaneously sense glutamate released into the extracellular volume. An alternative, although not mutually exclusive, hypothesis is that a pair of synchronized SICs derives from two synchronous episodes of glutamate release from two distinct sites, of the same or different astrocytes impinging on the two neurons. These two release episodes can be triggered by an $[Ca^{2+}]_i$ elevation occurring simultaneously in two astrocytic processes from the same or from two different astrocytes.

The presence of glutamate release sites in astrocytes at different distances from the recorded neuron could account for the variability in the rise and decay times of SICs. Additionally, the observation that two or more SICs recorded in the same neuron can have strikingly different kinetics suggests the presence of multiple release sites, from either one or many astrocytes impinging onto an individual CA1 neuron.

The complexity of astrocyte-to-neuron communication that emerges from these observations is further emphasized by the results obtained in confocal microscopy experiments in which $[Ca^{2+}]_i$ elevations triggered by astrocytic glutamate were observed to occur simultaneously in two to twelve CA1 neurons. An $[Ca^{2+}]_i$ elevation occurring in a solitary neuron was rare. This suggests that activation of multiple neurons by astrocytic glutamate is a common feature of this form of astrocyte-neuron crosstalk. With respect to the percentage of synchronized $[Ca^{2+}]_i$ elevations in neurons (75%), the percentage of synchronized SICs is apparently lower (23%). This discrepancy is most likely due to the fact that, in confocal microscopy experiments, we can image the Ca^{2+} response of tens of neurons simultaneously and thus have, with respect to paired recording experiments, a higher probability of observing a synchronized response in any two neurons in the field.

Importantly, SICs as well as synchronized $[Ca^{2+}]_i$ elevations in neuronal domains were also observed when $[Ca^{2+}]_i$ oscillations in astrocytes were triggered by intense stimulation of SCs. This observation suggests that when neuronal activity is high, activated astrocytes can signal back to neurons and synchronize activity in distinct neuronal domains. Such a response may represent a physiological signaling mode of astrocyte-to-neuron communication in the brain. The recent evidence for the presence of $[Ca^{2+}]_i$ oscillations in astrocytes in vivo (Hirase et al., 2004) underlines the importance of neuron-astrocyte interactions in brain function. While episodes of high neuronal activity similar to those that in our experiments activate the astrocyte response are commonly used to study the plasticity of synaptic transmission in brain slices (Bliss and Collingridge, 1993; Humeau et al., 2003; Malinow et al., 2000; Wang et al., 2003), it is conceivable that they might not be comparable to those that occur under physiological conditions in vivo. Future experiments should elucidate this issue. Activation of astrocytes by neuronal activity triggered domain responses in neurons also in the presence of 1 mM Mg^{2+}, although with a reduced probability compared to those from experiments that were carried out in the absence of Mg^{2+}. Furthermore, activation of astrocytes in 1 mM Mg^{2+} by DHPG, PGE_2, or neuronal activity still activates SICs. These observations further emphasize the physiological relevance of this form of astrocyte-to-neuron signaling.

This ability of astrocytic glutamate to activate NMDARs at a physiological concentration of Mg^{2+} was similarly observed in the ventrobasal thalamus (Parri et al., 2001). While the mechanism leading to the removal of the Mg^{2+} block is unclear, several possibilities can be proposed. For example, in addition to glutamate, astrocytes release D-serine (Schell et al., 1995), an effective ligand for the glycine binding site of the NMDA receptor, which may enhance the opening of the channel. Other factors released from astrocytes, such as ATP (Guthrie et al., 1999), may contribute to the removal of the Mg^{2+} block by depolarizing the neuronal membrane. Furthermore, since activation of the mGluR1 triggers membrane depolarization, an action of astrocytic glutamate on this neuronal receptor may also contribute. After the discovery that astrocytes can be activated by synaptic release of various neurotransmitters and have the ability to release neuroactive molecules, such as glutamate (Bezzi et al., 1998; Haydon, 2001; Parpura et al., 1994; Pasti et al., 1997) and ATP (Guthrie et al., 1999), several studies revealed at least some of the functional roles which may be ascribed to the reciprocal communication between these glial cells and neurons, including the control of the neurovascular coupling (Zonta et al., 2003) and the modulation of inhibitory transmission in the hippocampus (Kang et al., 1998; Liu et al., 2004). In the same brain region, astrocytic glutamate mediates an increase in the probability of spontaneous glutamate release from glutamatergic axon terminals, by acting on extrasynaptic mGluR receptors (Fiacco and McCarthy, 2004). This latter finding also supports our hypothesis of a preferential action of astrocytic glutamate on extrasynaptic receptors. The results we report reveal a hitherto unrecognized role of astrocytes in promoting coordinated activity of distinct subsets of CA1 pyramidal neurons.

Synchronization of neuronal activity is hypothesized to be of fundamental relevance to information processing in the brain (Singer, 1999). Although no consensus has yet emerged regarding its cellular mechanism, synchrony is believed to arise from the convergence of excitatory synaptic inputs and inhibitory interactions within the neuronal network (Harris et al., 2003). We show here that NMDAR activation by astrocytic glutamate represents an additional mechanism for neuronal synchrony. This mechanism can be operative under selected conditions, when more intense synaptic activity can increasingly activate the release of glutamate from astrocytes (Pasti et al., 1997). By cooperating with the excitatory synaptic inputs to recruit specific subsets of neurons in the neuronal network, the activation of extrasynaptic NMDA receptors by astrocytic glutamate may represent a flexible, additional mechanism that favors the formation of dynamically associated assemblies of neurons.

While this NMDA receptor-mediated signaling between astrocytes and neurons may contribute to the overall dynamics of neuronal synchrony, its very presence raises a series of questions on its possible role in pathological changes in the hippocampus, such as excitotoxic neuronal damage (Choi, 1988) or the generation of epileptiform activity (Dingledine et al., 1990).

In conclusion, we reveal that glutamate released from astrocytes acts on extrasynaptic NMDA receptors to promote synchronized activity in distinct neuronal domains in the CA1 hippocampal region. These results raise the possibility that astrocytes contribute to the formation of the basal functional module in brain information processing.

Experimental Procedures

Slice Preparation

Transverse hippocampal slices (300–400 μm) were prepared from Wistar rats at postnatal days 10–22 as described (Edwards et al., 1989; Pasti et al., 1997). Slices were cut with a Leica VT1000S vibratome and incubated at 37°C for a recovery period of at least 1 hr. All experiments were performed within 3 hr after the recovery. The physiological saline for slice cutting and incubation was NaCl, 120 mM; KCl, 3.2 mM; NaH_2PO_4, 1 mM; $NaHCO_3$, 26 mM; $MgCl_2$, 2 mM; $CaCl_2$, 1 mM; glucose, 2.8 mM; Na-pyruvate, 2 mM; and ascorbic acid, 0.6 mM at pH 7.4 with O_2 95%, CO_2 5%. In the experiments that used picrotoxin to block GABAergic inhibition (see below), the connection between the CA3 and CA1 regions was cut to overcome the spreading of epileptic-like activity. Slices for confocal microscopy were loaded with the Ca^{2+} indicator indo-1/AM (Molecular Probes, Eugene, OR) and 0.02% pluronic for 50 min under mild stirring at 37°C. Slice incubation with TeNT (2 μM, for 2 hr) was carried out at 37°C in a saline without Na-pyruvate and ascorbic acid.

Patch-Clamp Recordings and Analysis

Slices were put in the recording chamber and continuously perfused with NaCl, 120 mM; KCl, 3.2 mM; NaH_2PO_4, 1 mM; $NaHCO_3$, 26 mM; $CaCl_2$, 2 mM; glucose, 2.8 mM; glycine, 1 mM; at pH 7.4 with O_2 95%, CO_2 5%. The experiments in Figures 7 and 8 were performed in the presence of 1 mM Mg^{2+} in the recording saline. Unless otherwise specified, picrotoxin (100 μM, Sigma) was added to the saline to block $GABA_a$-mediated inhibition. Low Ca^{2+} solution was obtained by replacing $CaCl_2$ with EGTA (0.25 mM). Typical pipette resistance was 3–4 MΩ. Intracellular pipette solution was K-Gluconate, 145 mM; $MgCl_2$, 2 mM; EGTA, 5 mM; Na_2ATP, 2 mM; NaGTP, 0.2 mM; HEPES, 10 mM; to pH 7.2 with KOH. Patch-clamp recordings were performed using standard procedures and one or two Axopatch-200B amplifiers (Axon Instruments, Union City, CA). Data were fil-

tered at 1 KHz and sampled at 5 KHz with a Digidata 1200 interface and pClamp software (Axon instruments). Neurons were voltage clamped at −60 mV, unless otherwise stated. Evoked postsynaptic currents were triggered using a bipolar tungsten electrode (FHC, Bowdoinham, ME) positioned at the stratum radiatum to stimulate the SC pathway, 100–200 μm from the cell of interest. Single pulses (100 μs duration, 0.2–1 mA) were applied at 0.2 Hz. To study evoked synaptic tranmission in slices incubated with TeNT, the intensity of the stimulus applied to neuronal afferents was increased to 5–10 mA. To trigger SICs, stimuli were delivered to SCs at 25–30 Hz (100 or 200 ms duration trains repeated at 0.3 or 1 Hz for 10–30 s, 0.2–0.5 mA). Experiments were performed either at room temperature or at 35°C. Data analysis and fitting were performed with Clampfit 8.2 (Axon instrument) and Origin 6.0 (Microcal Software, Northampton, MA) software. The amplitude of both SICs and EPSCs was measured at the peak; rise time was calculated with the 20%–80% criterion, and the decay time as the time constant of a single or double exponential fit. Inward currents with rise time slower than 10 ms and amplitude greater than −20 pA were classified as SICs. SICs with an amplitude smaller than −20 pA or rise time faster than 10 ms were analyzed only when they occurred synchronously in neurons from the pair recording experiments. Due to the difficulty in applying a reliable kinetic analysis, some of these events were only considered for the calculation of the mean amplitude. Cells displaying an increased number of SICs during the period of stimulation with respect to an equal time period before stimulation were considered responsive. The frequency of spontaneous SICs was measured in these responsive neurons. The interevent time interval between two SICs was calculated as the time interval between the onset of the current in cell 1 and the onset of the current in cell 2. Data are expressed as mean ± SEM. Predictions obtained by a Monte Carlo simulation or by analysis of the Poisson distribution were used to estimate the probability of randomly occurring coincident SICs in our paired recordings. If the events are noncorrelated and occur randomly, the probability of each event is independent of the state of the other, and the probability density D of SICs in each neuron is estimated by N/T (N = total number of events recorded in the observation period T) and is time independent. The probability that n events occur in the time window τ is given by the Poisson distribution $p(n) = \exp(-D \times \tau) \times (D \times \tau)^{n/n!}$ and is plotted in the figure for both $n = 1$ and $n \geq 1$. We verified this prediction by simulating the random arrival of events on two channels with probability density of 0.0075 event/s by means of a Monte Carlo method. The probability of the simultaneous occurrence of two events as a function of the amplitude of the coincidence window is in agreement with the Poisson model and it is also plotted in the figure.

Confocal Microscopy

A confocal microscope (Nikon RCM8000) was used for monitoring the $[Ca^{2+}]_i$ change at the single-cell level as previously described (Pasti et al., 1997). Slices were continuously perfused with the same extracellular solution that was used in electrophysiological recording with sulfinpyrazone (0.2 mM). The sampling rate was 1–4 s and 16 to 32 images were averaged for each frame. To activate $[Ca^{2+}]_i$ elevations in astrocytes, we used the same stimulation protocol that in patch-clamp experiments triggered SICs. Experiments were performed at either room temperature or 35°C. Cells in the focal plane 10–30 μm beneath the surface of the slice were monitored. Cells located at different depths displayed a similar value of R405/485, indicating that the neurons and astrocytes under study were not damaged by slicing procedures. Neurons and astrocytes were distinguished on the basis of the distinct kinetics of their response to high K^+ stimulation, which, as previously reported (Pasti et al., 1997), was always performed at the end of the experiment. The maximal extension of the neuronal domain that displayed a synchronized response was estimated as the distance between the centers of the somata of the two neurons positioned at the borders of the responsive domain. The interevent time interval of $[Ca^{2+}]_i$ elevations in neurons was estimated by comparing the timing for the $[Ca^{2+}]_i$ response from each responsive neuron within a time window of 12 s. In the experiments that used an acquisition time interval of 1 or 2 s, responses were classified as synchronous when they occurred at the same time frame. The time interval between the astrocytic and the neuronal response is obtained by measuring the timing for the $[Ca^{2+}]_i$ elevation in each astrocyte with respect to that for the $[Ca^{2+}]_i$ elevation in each neuron of the field.

Photolysis

In some experiments, photolysis was performed in conjunction with wide-field fluorescence imaging and electrophysiology. Similar approaches to those discussed above were used but employed 8–13 day Swiss Webster mice. Since SICs that were similar in properties to those detected in rat slices were seen in recordings from these murine slices in response to activation of metabotropic receptors (data not shown), we pooled data from both of these rodents in this study. Hippocampal slices were prepared as detailed previously (Sul et al., 2004), and astrocytes were bulk loaded for 2 hr at room temperature in ACSF containing fluo-4 AM (12.5 μg/ml), NP-EGTA (25 μg/ml), DMSO (0.1%), and pluronic (0.05%) saturated with O_2 95%, CO_2 5%. Since greater than 98% of the calcium indicator-loaded cells were astrocytes, we used the presence of the indicator loading to determine cell identity (Sul et al., 2004). Parallel whole-cell recordings confirmed cell identity. CA1 neurons from such slices were recorded with the patch-clamp technique using an Axoclamp amplifier 1C. Pipettes had a resistance of 4–5 MΩ when loaded with a solution containing K-Gluconate, 130 mM; $CaCl_2$, 1 mM; $MgCl_2$, 2 mM; EGTA, 11 mM; MgATP, 1.5 mM; NaGTP, 0.3 mM; HEPES, 10 mM; to pH 7.2 with KOH. The fluorescent dye Alexa 568 (0.1 mM) (Molecular Probes) was added to this solution to visualize the dendrites of the recorded neuron. Photorelease of Ca^{2+} was performed by a 3 μm diameter UV pulse (351 and 364 nm) generated by an argon ion laser (Coherent Enterprise II; duration 100 ms, power 200–250 μW) connected by an optical fiber to an Uncager system (Prairie Technologies, Inc., Middleton, WI). Images were acquired using a Q imaging cooled CCD camera and Image-Pro software. The UV pulse, camera acquisitions, and electrophysiology were all controlled by pClamp software (version 9.0; Axon Instruments) connected to a Digidata 1332A. Analysis of the images was performed using Metamorph software (Universal Imaging Corp., Downingtown, PA).

Drugs

DHPG, CHPG, D-AP5, MK-801, NBQX, cyclothiazide, DL-TBOA, and LY 367385 were obtained from Tocris Cookson (Buckhurst Hill, UK); ifenprodil, GDP-β-S, ATP, Bz-ATP, and α,β-methylen-ATP were from Sigma (Milan, Italy); PGE_2 was from Biomol (Plymouth Meeting, PA). Purified TeNT was kindly provided by Dr. O. Rossetto, Department of Experimental Biomedical Sciences, University of Padova, Padova, Italy.

Acknowledgments

We thank Micaela Zonta for helpful discussion and for the preparation of figures and movies; Maria Cecilia Angulo for performing some experiments in an initial stage of our study; Gian Michele Ratto for simulation analysis; and Yolande Haydon for editing our manuscript. This work was supported by grants from the Armenise-Harvard University Foundation, the Italian University and Health Ministries (FIRB, RBNE01RHZM_003) and ST/Murst: "Neuroscienze" to G.C., the Italian Association for Cancer Research (AIRC), and European Community (QLG3-CT-2000-00934) to T.P., and the NIH (RO1 NS43142; R37 NS37585; P20-MH-071705) (to P.G.H.). The authors of this paper have declared a conflict of interest. For details, go to http://www.neuron.org/cgi/content/full/43/5/729/DC1.

Received: February 24, 2004
Revised: July 26, 2004
Accepted: August 6, 2004
Published: September 1, 2004

References

Araque, A., Li, N., Doyle, R.T., and Haydon, P.G. (2000). SNARE protein-dependent glutamate release from astrocytes. J. Neurosci. *20*, 666–673.

Arcuino, G., Lin, J.H.-C., Takano, T., Liu, C., Jiang, L., Gao, Q.,

Kang, J., and Nedergaard, M. (2002). Intercellular calcium signaling mediated by point-source burst release of ATP. Proc. Natl. Acad. Sci. USA *99*, 9840–9845.

Attwell, D., Barbour, B., and Szatkowski, M. (1993). Nonvesicular release of neurotransmitter. Neuron *11*, 401–407.

Bezzi, P., Carmignoto, G., Pasti, L., Vesce, S., Rossi, D., Rizzini, B.L., Pozzan, T., and Volterra, A. (1998). Prostaglandins stimulate calcium-dependent glutamate release in astrocytes. Nature *391*, 281–285.

Bezzi, P., Gundersen, V., Galbete, J.L., Seifert, G., Steinhäuser, C., Pilati, E., and Volterra, A. (2004). Astrocytes contain a vesicular compartment that is competent for regulated exocytosis of glutamate. Nat. Neurosci. *7*, 613–620.

Bliss, T.V.P., and Collingridge, G.L. (1993). A synaptic model of memory: long-term potentiation in the hippocampus. Nature *361*, 31–39.

Bourne, H.R., and Nicoll, R. (1993). Molecular machines integrate coincident synaptic signals. Cell Suppl. *72*, 65–75.

Carmignoto, G. (2000). Reciprocal communication systems between astrocytes and neurones. Prog. Neurobiol. *62*, 561–581.

Choi, D.W. (1988). Glutamate neurotoxicity and diseases of the nervous system. Neuron *1*, 623–634.

Choi, D.W., and Rothman, S.M. (1990). The role of glutamate neurotoxicity in hypoxic-ischemic neuronal death. Annu. Rev. Neurosci. *13*, 171–182.

Congar, P., Leinekugel, X., Ben-Ari, Y., and Crépel, V. (1997). A long-lasting calcium-activated nonselective cationic current is generated by synaptic stimulation or exogenous activation of group I metabotropic glutamate receptors in CA1 pyramidal neurons. J. Neurosci. *17*, 5366–5379.

Constantine-Paton, M., Cline, H.T., and Debski, E. (1990). Patterned activity, synaptic convergence, and the NMDA receptor in developing visual pathways. Annu. Rev. Neurosci. *13*, 129–154.

Conti, F., and Weinberg, R.J. (1999). Shaping excitation at glutamatergic synapses. Trends Neurosci. *22*, 451–458.

Crépel, V., Aniksztejn, L., Ben-Ari, Y., and Hammond, C. (1994). Glutamate metabotropic receptors increase a Ca^{2+}-activated nonspecific cationic current in CA1 hippocampal neurons. J. Neurophysiol. *72*, 1561–1569.

Diamond, J.S., and Jahr, C.E. (1995). Asynchronous release of synaptic vesicles determines the time course of the AMPA receptor-mediated EPSC. Neuron *15*, 1097–1107.

Dingledine, R., McBain, C.J., and McNamara, J.O. (1990). Excitatory amino acid receptors in epilepsy. Trends Pharmacol. Sci. *11*, 334–338.

Dingledine, R., Borges, K., Bowie, D., and Traynelis, S.F. (1999). The glutamate receptor ion channels. Pharmacol. Rev. *51*, 7–61.

Edwards, F.A., Konnerth, A., Sakmann, B., and Takahashi, T. (1989). A thin slice preparation for patch clamp recordings from neurones of the mammalian central nervous system. Pflugers Arch. *414*, 600–612.

Fellin, T., and Carmignoto, G. (2004). Neuron-to-astrocyte signaling in the brain represents a distinct multifunctional unit. J. Physiol. *559*, 3–15.

Fiacco, T.A., and McCarthy, K.D. (2004). Intracellular astrocyte calcium waves *in situ* increase the frequency of spontaneous AMPA receptor currents in CA1 pyramidal neurons. J. Neurosci. *24*, 722–732.

Guthrie, P.B., Knappenberger, J., Segal, M., Bennett, M.V., Charles, A.C., and Kater, S.B. (1999). ATP released from astrocytes mediates glial calcium waves. J. Neurosci. *19*, 520–528.

Hardingham, G.E., Fukunaga, Y., and Bading, H. (2002). Extrasynaptic NMDARs oppose synaptic NMDARs by triggering CREB shut-off and cell death pathways. Nat. Neurosci. *5*, 405–414.

Harris, K.D., Csicsvari, J., Hirase, H., Dragoi, G., and Buzsáki, G. (2003). Organization of cell assemblies in the hippocampus. Nature *424*, 552–556.

Haydon, P.G. (2001). GLIA: listening and talking to the synapse. Nat. Rev. Neurosci. *2*, 185–193.

Hirase, H., Qian, L., Barthó, P., and Buzsáki, G. (2004). Calcium dynamics of cortical astrocytic networks in vivo. PLoS Biol. 2(4): e96 DOI: 10.1371/journal.pbio.0020096.

Humeau, Y., Shaban, H., Bissière, S., and Lüthi, A. (2003). Presynaptic induction of heterosynaptic associative plasticity in the mammalian brain. Nature *426*, 841–845.

Kang, J., Jiang, L., Goldman, S.A., and Nedergaard, M. (1998). Astrocyte-mediated potentiation of inhibitory synaptic transmission. Nat. Neurosci. *1*, 683–692.

Kullmann, D.M. (1999). Synaptic and extrasynaptic roles of glutamate in the mammalian hippocampus. Acta Physiol. Scand. *166*, 79–83.

Liu, Q.-S., Xu, Q., Arcuino, G., Kang, J., and Nedergaard, M. (2004). Astrocyte-mediated activation of neuronal kainate receptors. Proc. Natl. Acad. Sci. USA *101*, 3172–3177.

Malinow, R., Mainen, Z.F., and Hayashi, Y. (2000). LTP mechanisms: from silence to four-lane traffic. Curr. Opin. Neurobiol. *10*, 352–357.

Matthias, K., Kirchhoff, F., Seifert, G., Hüttmann, K., Matyash, M., Kettenmann, H., and Steinhäuser, C. (2003). Segregated expression of AMPA-type glutamate receptors and glutamate transporters defines distinct astrocyte populations in the mouse hippocampus. J. Neurosci. *23*, 1750–1758.

Parpura, V., Basarsky, T.A., Liu, F., Jeftinija, K., Jeftinija, S., and Haydon, P.G. (1994). Glutamate-mediated astrocyte-neuron signalling. Nature *369*, 744–747.

Parri, H.R., Gould, T.M., and Crunelli, V. (2001). Spontaneous astrocytic Ca^{2+} oscillations in situ drive NMDAR-mediated neuronal excitation. Nat. Neurosci. *4*, 803–812.

Pasti, L., Volterra, A., Pozzan, T., and Carmignoto, G. (1997). Intracellular calcium oscillations in astrocytes: a highly plastic, bidirectional form of communication between neurons and astrocytes in situ. J. Neurosci. *17*, 7817–7830.

Pasti, L., Zonta, M., Pozzan, T., Vicini, S., and Carmignoto, G. (2001). Cytosolic calcium oscillations in astrocytes may regulate exocytotic release of glutamate. J. Neurosci. *21*, 477–484.

Patneau, D.K., and Mayer, M.L. (1990). Structure-activity relationships for amino acid transmitter candidates acting at N-methyl-D-aspartate and quisqualate receptors. J. Neurosci. *10*, 2385–2399.

Porter, J.T., and McCarthy, K.D. (1996). Hippocampal astrocytes in situ respond to glutamate released from synaptic terminals. J. Neurosci. *16*, 5073–5081.

Rumbaugh, G., and Vicini, S. (1999). Distinct synaptic and extrasynaptic NMDA receptors in developing cerebellar granule neurons. J. Neurosci. *19*, 10603–10610.

Schell, M.J., Molliver, M.E., and Snyder, S.H. (1995). D-serine, an endogenous synaptic modulator: localization to astrocytes and glutamate-stimulated release. Proc. Natl. Acad. Sci. USA *92*, 3948–3952.

Schiavo, G., Benfenati, F., Poulain, B., Rossetto, O., Polverino de Laureto, P., DasGupta, B.R., and Montecucco, C. (1992). Tetanus and botulinum-B neurotoxins block neurotransmitter release by proteolytic cleavage of synaptobrevin. Nature *359*, 832–835.

Scimemi, A., Fine, A., Kullmann, D.M., and Rusakov, D.A. (2004). NR2B-containing receptors mediate cross talk among hippocampal synapses. J. Neurosci. *24*, 4767–4777.

Shimamoto, K., Lebrun, B., Yasuda-Kamatani, Y., Sakaitani, M., Shigeri, Y., Yumoto, N., and Nakajima, T. (1998). DL-threo-beta-benzyloxyaspartate, a potent blocker of excitatory amino acid transporters. Mol. Pharmacol. *53*, 195–201.

Singer, W. (1999). Neuronal synchrony: a versatile code for the definition of relations? Neuron *24*, 49–65.

Stocca, G., and Vicini, S. (1998). Increased contribution of NR2A subunit to synaptic NMDA receptors in developing rat cortical neurons. J. Physiol. *507*, 13–24.

Sul, J.-Y., Orosz, G., Givens, R.S., and Haydon, P.G. (2004). Astrocytic connectivity in the hippocampus. Neuron Glia Biol. *1*, 3–11.

Tovar, K.R., and Westbrook, G.L. (1999). The incorporation of NMDA receptors with a distinct subunit composition at nascent hippocampal synapses in vitro. J. Neurosci. *19*, 4180–4188.

Tovar, K.R., and Westbrook, G.L. (2002). Mobile NMDA receptors at hippocampal synapses. Neuron *34*, 255–264.

Ventura, R., and Harris, K.M. (1999). Three-dimensional relationships between hippocampal synapses and astrocytes. J. Neurosci. *19*, 6897–6906.

Wang, Z., Xu, N.-L., Wu, C.-P., Duan, S., and Poo, M.-M. (2003). Bidirectional changes in spatial dendritic integration accompanying long-term synaptic modifications. Neuron *37*, 463–472.

Williams, K. (1993). Ifenprodil discriminates subtypes of the N-methyl-D-aspartate receptor: selectivity and mechanisms at recombinant heteromeric receptors. Mol. Pharmacol. *44*, 851–859.

Yamada, K.A., and Tang, C.-M. (1993). Benzothiadiazides inhibit rapid glutamate receptor desensitization and enhance glutamatergic synaptic currents. J. Neurosci. *13*, 3904–3915.

Zanotti, S., and Charles, A. (1997). Extracellular calcium sensing by glial cells: low extracellular calcium induces intracellular calcium release and intercellular signaling. J. Neurochem. *69*, 594–602.

Zonta, M., Angulo, M.C., Gobbo, S., Rosengarten, B., Hossmann, K.-A., Pozzan, T., and Carmignoto, G. (2003). Neuron-to-astrocyte signaling is central to the dynamic control of brain microcirculation. Nat. Neurosci. *6*, 43–50.